International Journal of Surgical Pathology
2014, Vol. 22(4) 303–315

DOI: 10.1177/1066896913503491
ijs.sagepub.com
SAGE

Topographic Distribution of Papillary Thyroid Carcinoma by Mapping in Coronal Sections of 125 Consecutive Thyroidectomy Specimens

Kien T. Mai, MD[1], Previn Gulavita, MD[1], Chi Lai, MD[1], Joanne Swift, MLT[1], Joelle Levac, MLT[1], Bernhard Olberg, MD[1], and Bibianna Purgina, MD[1]

Abstract

Introduction. Mapping of different foci in multifocal papillary thyroid carcinoma (PTC) has previously not been done as it is difficult to do so when thyroid specimens are serially sectioned transversely (ie, parallel to the horizontal plane). In this study, thyroidectomy specimens were serially sectioned coronally (ie, parallel to the largest surface of the thyroid gland), which allows for panoramic and 3-dimensional visualization of PTC foci and their relationship to one another. *Materials and methods*. A total of 125 consecutive total thyroidectomies or lobectomies followed by completion thyroidectomies were serially sectioned coronally and reviewed with identification and characterization of PTC foci. PTCs were grouped into either discrete, encapsulated nodule(s) (EN) of both follicular or papillary architecture, usual variant (UV), or tall cell variant (TCV). *Results*. The predominant tumor masses were identified in the right lobe, isthmus, and left lobe in 52%, 8%, and 40%, respectively. The largest tumor nodules ranged from 3 to 60 mm (18.8 ± 6.6) with the UV, EN, and TCV groups accounting for 58%, 24%, and 18% of cases, respectively. Three topographic patterns of PTC can be distinguished as follows: (*a*) single tumor nodule (37 cases), (*b*) main tumor nodule with satellite nodule(s) displaying no or varying degrees of fusion with the main one (30 cases), and (*c*) main tumor nodule with either a second large nodule or randomly occurring tumor nodules (58 cases). Bilaterality can be seen in all 3 patterns but was most prevalent in the group comprising the main tumor nodule with either a second large nodule or random tumor nodules. It was least frequent in the EN group without random tumor nodules. The difference in rates of bilaterality between tumors <10 mm and ≥10 mm was statistically significant ($P < .01$). For all 3 groups, satellite nodules displayed histopathological features that were similar or dissimilar to the main tumor mass. They may be of a different variant than that of the main tumor nodule. *Conclusions*. With panaromic and 3-dimensional visualization, individual tumors/satellite or random nodules of multifocal PTC were readily identified in serial coronal sections of thyroidectomy specimens. Bilaterality was frequently observed in tumors associated with random PTC foci, whereas, the EN group tended to be unilateral and was not associated with random foci.

Keywords

thyroid, carcinoma, papillary, mapping

Introduction

Well-differentiated papillary thyroid carcinoma (PTC) is the most common malignancy of the endocrine organs. In many industrialized countries, there is a consistent increase in the frequency of thyroid cancer, which is not only because of environmental causes but also because of changes in diagnostic techniques and pathological criteria.[1-7] Multifocal and bilateral involvement of the thyroid gland and frequent lymph nodal metastasis are hallmarks of PTC. Most thyroid cancers are highly treatable and curable with surgery alone or in combination with other treatments. Multifocality and bilaterality are variable from case to case, and often unpredictable. Recent molecular techniques with clonal studies have elucidated to some extent the role of intraglandular spread as a mechanism of

[1]The Ottawa Hospital and Ottawa University, Ottawa, Ontario, Canada

Corresponding Author:
Kien T. Mai, Department of Pathology & Laboratory Medicine, The Ottawa Hospital, General Campus, 501 Smyth Road, Ottawa, Ontario, K1H 8L6, Canada.
Email: ktmai@ottawahospital.on.ca

multifocality.[8,9] However, other studies support the development of independent foci with different clones of PTC, thus favoring multicentricity.[10-12] The latter is further supported by the difficulty in identification of intraglandular lymphatic invasion in thyroid tissue harboring PTC and the cytohistomorphological diversity of multicentric PTC.[12] Study of the topographic distribution of PTC foci may be helpful to characterize the differential distribution patterns of multifocal PTC as well as to elucidate the mechanism of multifocality and to enhance our understanding of tumor progression. However, topographic mapping of different PTC foci has previously not been performed as it is often limited by the current technique of tissue sampling with serial transverse sectioning (parallel to horizontal plane) of the thyroid that tends to divide tumor foci into multiple sections. In this study, topographic mapping with panoramic visualisation of PTC foci in thyroid specimens sectioned in a plane parallel to the largest surface of the gland (coronal plane) was performed.

Materials and Methods

Thyroid specimens (total thyroidectomies or lobectomies followed by completion thyroidectomies) were fixed in 10% neutral buffered formalin. After inking the outer surfaces (left lobe, green; isthmus, yellow; right lobe, black), the entire gland or lobe was serially sectioned coronally into 3- to 5-mm slices. Care was taken so that at least one giant section of the entire specimen was obtained. Depending on the anterior-posterior diameter of the specimen, at least 2 (when available) or alternate giant sections were selected for microscopic examination by dividing them into smaller sections using a grid pattern. The most anterior and posterior giant sections were serially sectioned transversely in order to visualize the inked resection margins on microscopic sections. All giant sections were photographed before being divided and all routine sections were properly recorded to enable the reconstruction of the giant sections at microscopic examination.

Consecutive specimens of total thyroidectomies or lobectomies followed by completion thyroidectomies sectioned in the coronal plane were reviewed with identification and characterization of PTC foci. PTC was diagnosed with current criteria and reviewed with consensus between 3 pathologists specialized in thyroid pathology. PTCs were grouped into encapsulated nodule(s) (EN) of both follicular or papillary architecture, usual variant (UV), and tall cell variant (TCV). The latter was defined as PTC that exhibited tall cell features in at least 50% of the tumor. Each group was stratified according to the maximum dimension into tumors measuring <10 mm, 10 to 20 mm, and >20 mm. Additional foci of PTC smaller than the largest tumor nodule were arbitrarily designated as either satellite or random nodules based on the distance from the main tumor nodule, that is, less or greater than 3 mm, respectively (approximately the thickness of the tissue block). Cases without complete or nearly complete (<80%) submission of thyroid tissue were excluded from the study. To simplify the study, diffuse sclerosing PTC were excluded from the study. All slides were screened for lymphovascular invasion. Areas with questionable lympho/vascular invasion and lympho versus vascular were reviewed by at least one of pathologists. In addition these areas were immunostained for CD31 (Dako, Glostrup, Denmark, Catalog M0823, dilution 1:100), CD34 (Leica MicroSystems, Richmond Hill, Ontario, Canada, Catalog No: PA0212; for vascular invasion) and D2-40 (Dako, Catalog M3619, dilution 1:100; for vascular invasion). Immunohistochemical staining was performed on formalin-fixed tissue sections using the BOND-MAX automated system (Leica). Statistical analysis was performed using SISA software.

Results

A total of 125 consecutive specimens comprising 77 UV, 30 EN, and 18 TCV were evaluated. The patient population exhibited a female predominance (3:1 ratio) with ages ranging from 23 to 76 years (54 ± 12 years). The predominant tumor masses were located in the right lobe, isthmus, and left lobe in 52%, 8%, and 40% of cases. Tumors ranged from 3 to 60 mm (18.8 ± 6.6 mm) with tumors <10 mm, 10 to 20 mm, and >20 mm accounting for 12, 39, and 26 cases of UV; 3, 7, and 20 cases of EN; and 4, 6, and 8 cases of TCV, respectively.

Table 1 shows the 3 PTC groups stratified into tumors measuring <10 mm, 10 to 20 mm, and >20 mm. These are further subcategorized according to the distribution pattern of the main tumor nodule and the smaller tumor foci as follows:

(a) Single tumor nodule in one lobe with or without contralateral foci (Figures 1 and 2)
(b) Single tumor nodule in one lobe associated with a satellite nodule or cluster of satellite nodules adjacent to the main tumor with or without contralateral foci (Figures 3 and 4)
(c) Single tumor nodule associated with a second large nodule greater than 1 cm in diameter, regard less location or random foci in one or both lobes with or without contralateral foci (Figures 5 and 6).

Also shown are the number of cases with bilateral disease, isthmus involvement, and lymph nodes metastases with follow-up of up to 30 months (25 ± 8 months). The difference in rates of bilaterality between single tumor nodule with or without adjacent satellite nodule(s) and second tumor nodule or random foci was statistically significant ($P < .01$).

Table 1. Topographic Distribution of Papillary Thyroid Carcinoma Foci According to Tumor Type.[a]

Number (Largest Tumor in mm)	Diameter (mm)	Single Tumor Nodule	Main Tumor Nodule With Satellite Nodule(s)	Main Tumor Nodule With Either Second Large Nodule or Random Tumor Nodules [Bilateral][b]	Total	Isthmus Involved in Bilaterality	Lymphatic Invasion	Lymph Nodal Metastasis (2-Year Follow-up)
UV 73	<10	8	2	2[1]	12[1]	1	0	1
(16.5 ± 4.6)	10-20	8 [1]	9[3]	22 [12]	39[16]	2	2 [1]	8
	>20	0	3	23[17]	26[17]	8	4 [2]	15
(Total)		(16) (21%) [1] [1.3%]	(14) (18%) [3] [4%]	(47) (61%) [30] [39%]	(77) (100%) [34] [44%]	11 (32.3%)[c]		24 (31.2%)
EN 30	<10	2	1	0	3	0	0	0
(28.4 ± 12)	10-20	4	2	1	7	0	0	0
	>20	12 [1]	5 [1]	3 [2]	20	0	0	1
(Total)		(18) (60.0%) [1] [3.3%]	(8) (26.7%) [1] [3.3%]	(4) (13.3%) [2] [6.7%]	(30) (100%) [4] [13.3%]	0		1 (3.3%)
TCV 22	<10	1	2	1 [1]	4 [1]	0	0	2
(13.7 ± 4.3)	10-20	2	2	2 [2]	6 [2]	2	2	5
	>20	0	3	5 [4]	8 [4]	2	3 [1]	8
(Total)		(3) (16.7%)	(7) (38.9%)	(8) (44.4%) [7] [38.9%]	(18) (100%) [7] [38.9%]	4 (57.1%)[c]		15 (83.4%)
Grand total		37 (29.6%) [2] [1.6%]	30 (24.0%) [3] [2.4%]	58 (46.4%) [39] [31.2%]	125 (100%) [44] [35%]	15 (34.1%)[c]	11 [4]	40 (32.0%)

Abbreviations: UV, usual variant; EN, encapsulated nodule; TCV, tall cell variant.

[a]The difference in rates of bilaterality between second large nodule or random foci and a single nodule with or without satellite nodule(s) was statistically significant ($P < .01$).

[b]Figure in brackets indicates number of cases with bilateral involvement.

[c]Percentage calculated from cases with bilateral involvement of the thyroid.

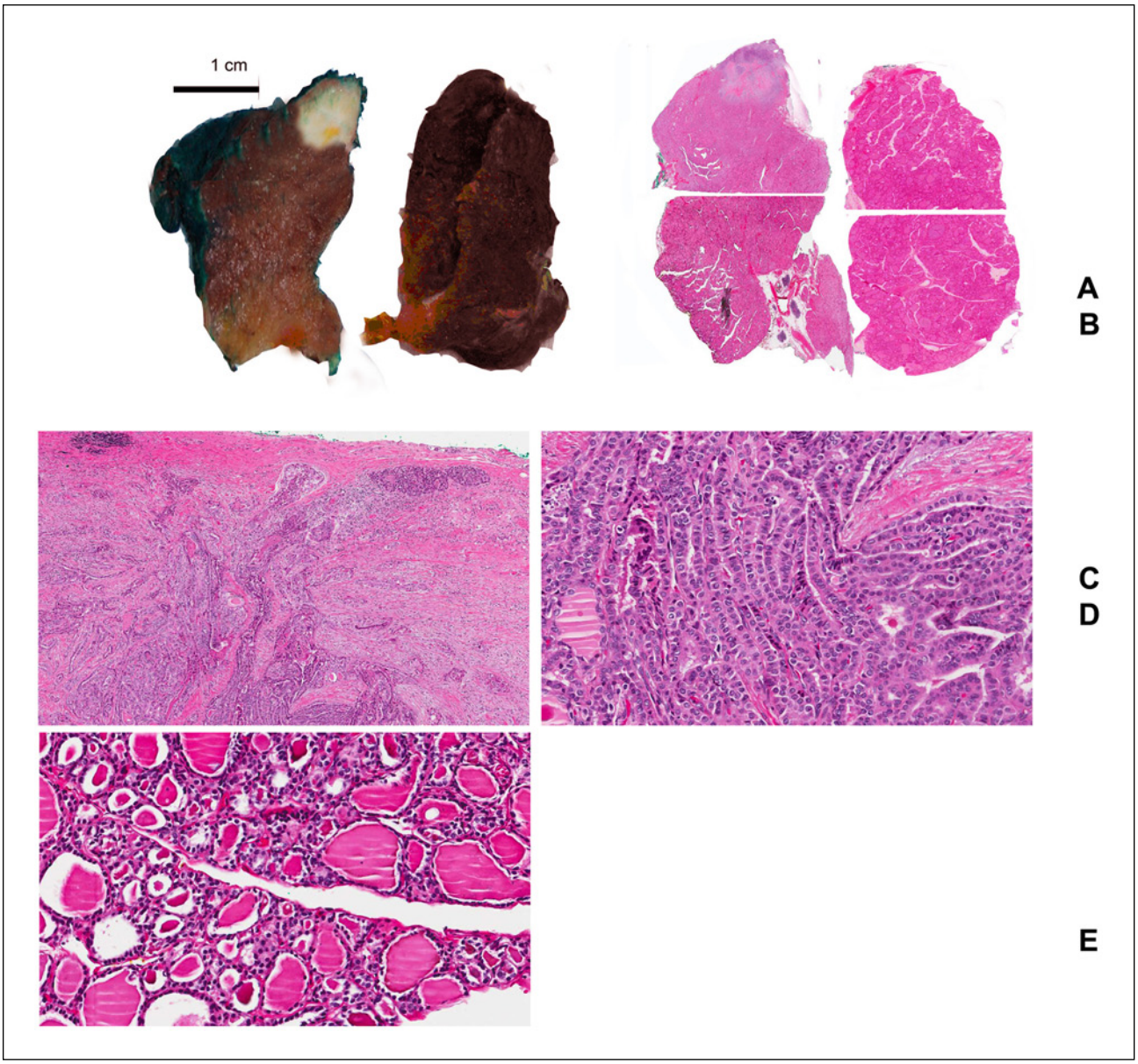

Figure 1. Lobectomy followed by a completion thyroidectomy: (A) A coronal section showing a single, 8-mm focus of tall cell variant (TCV). (B) Assembled hematoxylin and eosin–stained slides. (C) Low-power and (D) high-power magnification of TCV. (E) Normal thyroid tissue of the remaining tissue.

For the UV group, the mean tumor diameter was 16.5 ± 4.6 mm. This group was associated with the lowest rate of a single tumor nodule (21%), the highest rate of random foci in the gland (61%), and a higher rate of bilaterality (44%). The rate of isthmus involvement in bilateral disease was 32.3%. The rate of lymph node metastasis was 31%.

The EN group was associated with the largest tumor dimension of 28.4 ± 12 mm, the highest rate of a single tumor nodule (60%), the lowest rate of random foci in the gland (13%), the lowest rate of bilaterality (13%), and the lowest rate of lymph node metastasis (3.3%).

The TCV group demonstrated the smallest tumor size (13.7 ± 4.3 mm) but was associated with the highest rate of lymph nodal metastases (83.4%). Random foci within the specimen and bilaterality were observed in 44.4% and 38.9% of TCV cases, respectively. The rate of isthmus involvement in bilateral disease was 57% of TCV cases.

In the EN group, the main tumor accompanied by satellite nodules may pose diagnostic difficulty in distinguishing between multifocality and capsular invasion as well as a problem with accurate measurement of the tumor nodule (Figures 3 and 4). Lymphatic vessel invasion was

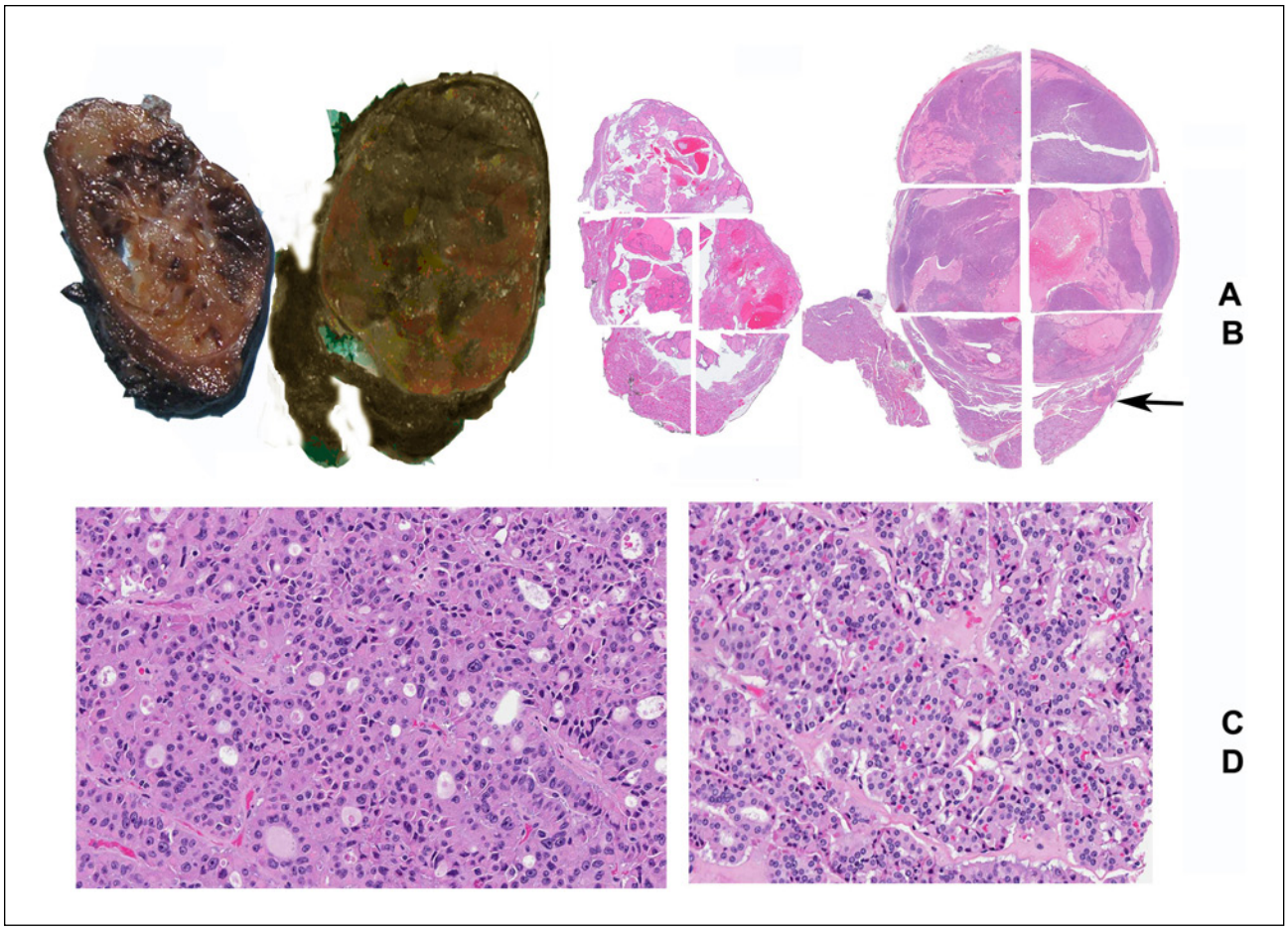

Figure 2. Total thyroidectomy for a single, large encapsulated nodule (EN), follicular type: (A) A coronal section showing an encapsulated tumor. (B) Assembled hematoxylina nd eosin–stained slides showing a large encapsulated follicular variant of papillary thyroid carcinoma (PTC) and hemorrhagic areas accompanied by one small satellite nodule (arrow) within a background of multinodular goiter with adenomatoid nodules on the contralateral side. (C) Focal areas with nuclear changes of PTC. (D) Satellite nodule (arrow in B) and contralateral: Follicular lesion with smaller nuclei with rather coarse chromatin.

identified in 0, 2, 4 and 0, 2, 3 in UV and TCV measuring <1 cm, <2 cm, and >2 cm, respectively all EV. Lymphatic vessel invasion was identified in 0, 1, 2 and 0, 0, 1 in UV and TCV with bilaterality measuring <1 cm, <2 cm, and >2 cm, respectively. No lymphatic invasion was seen in all EV cases.

Table 2 summarizes the distribution of PTC foci according to tumor size. The difference in rates of bilaterality between tumors <10 mm and >10 mm was statistically significant ($P < .01$). The difference in rates of lymph nodal metastases between tumors <10 mm and >10 mm was not statistically significant ($P = .1$).

Multifocal/multicentric tumors displayed either similar or different histopathological characteristic (oncocytic versus non oncocytic variant, common variant versus TCV, papillary versus follicular architecture of different types of PTC variant). Examination of areas adjacent to or even distant from the main tumor nodules in multifocal PTC was able to identify microscopic foci of poorly circumscribed follicular lesions that exhibited nuclear changes approaching but not up to the level of PTC.

Discussion

In this study, the gender ratio and patient ages were consistent with previously reported gender ratio and age distribution of PTC.[13,14] Of note, there was a slight predominance of PTC in the right thyroid lobe.

Recently, molecular studies have elucidated the carcinogenetic mechanisms of PTC.[15-34] Mutations in either BRAF or RAS genes or RET/PTC gene rearrangements have been found in greater than 70% of PTC.[16] BRAF mutation, the most common genetic alteration in PTC, is most commonly found in the classic and tall cell variants of PTC. It is rarely found in the follicular variant of PTC.[15,16] This mutation is associated with older patient age

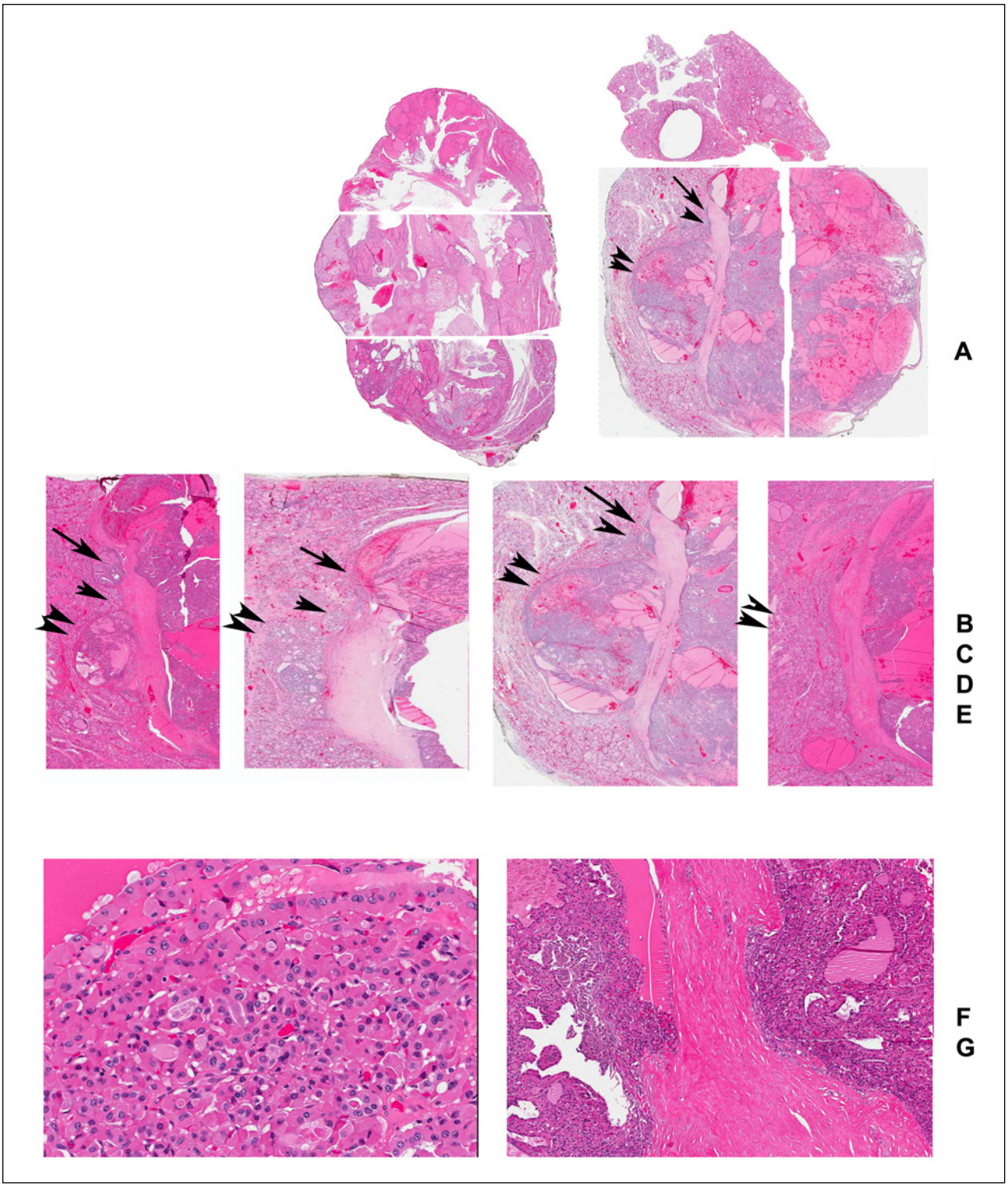

Figure 3. Total thyroidectomy for a multifocal encapsulated nodule (EN) of papillary thyroid carcinoma (PTC) with clusters of small PTC foci adjacent to the main tumor: (A) Assembled hematoxylin and eosin–stained slides showing a coronal section of both right and left lobe with an encapsulated follicular variant of PTC and adjacent cluster of 3 nodules of PTC (arrow, single arrowhead, and double arrowhead). (B, C, D, and E) Serial coronal sections showing the encapsulated, oncocytic follicular variant of PTC with 3 satellite foci (arrow, single arrowhead, and double arrowhead) mimicking tumor invasion through the capsule. (F) High magnification of oncocytic follicular variant of PTC. (G) Tumor on both sides attached to the thick capsule. Serial step sections did not reveal capsular penetration.

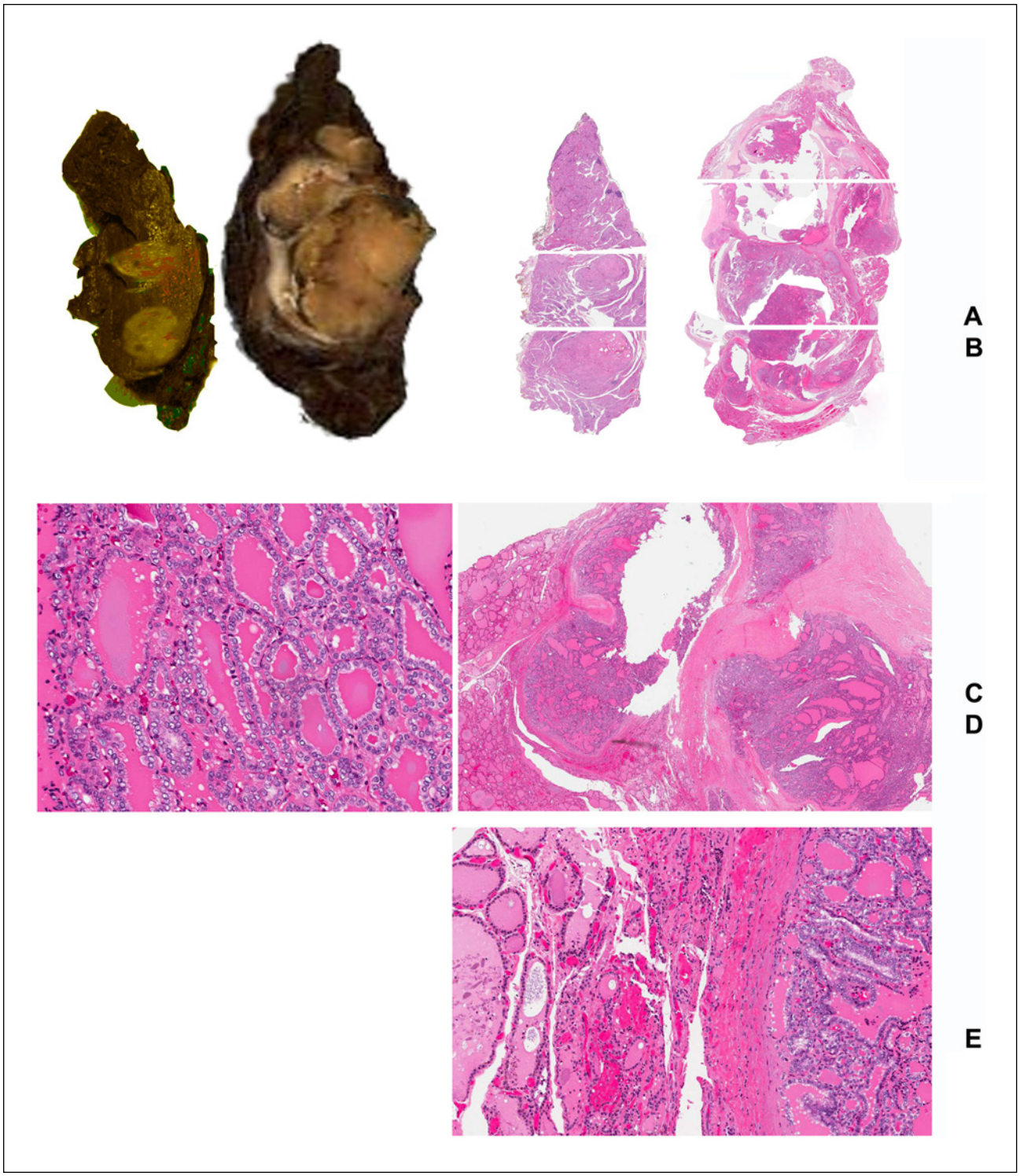

Figure 4. Total thyroidectomy for a large, encapsulated, and unilateral papillary thyroid carcinoma (PTC) with satellite PTC nodules adjacent to the main tumor. This tumor exhibited a similar topographic distribution to that in Figure 3; however, it had more remarkable nuclear changes and a thicker fibrous capsule: (A) Coronal sections showing lesional foci in the left thyroid lobe having the polycyclic contour. (B) Assembled hematoxylin and eosin–stained slides showing the largest tumor nodule surrounded by band of dense fibrous tissue and smaller, encapsulated satellite tumor nodules in the middle part the left lobe resulting in a composite tumor with a much greater dimension than the main tumor nodule. The right lobe displayed 2 adenomatoid nodules. (C) A high magnification of the main tumor nodule. (D) A low magnification of the encapsulated satellite PTC nodules. (E) A high magnification of a small PTC nodule.

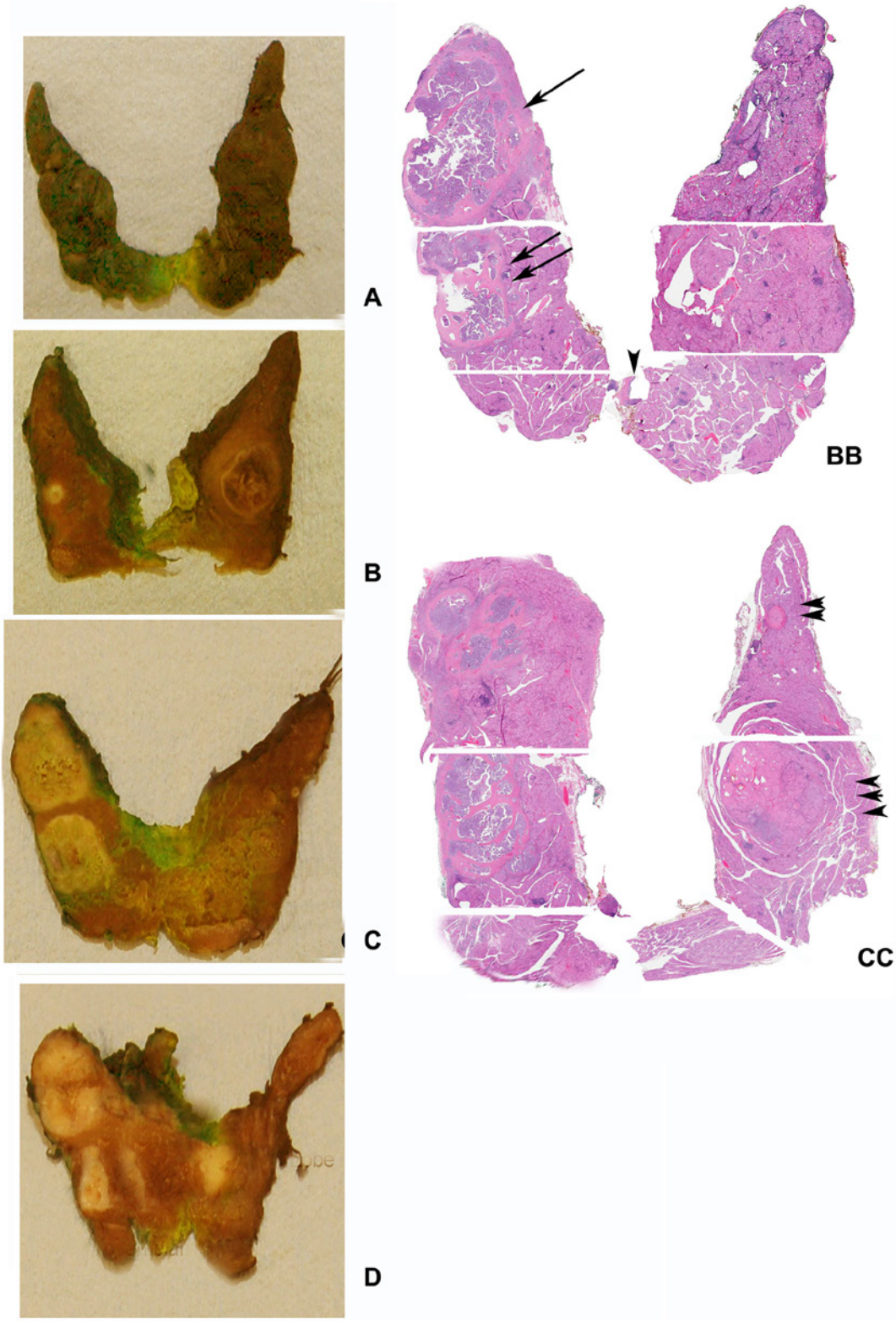

(continued)

Figure 5. (continued)

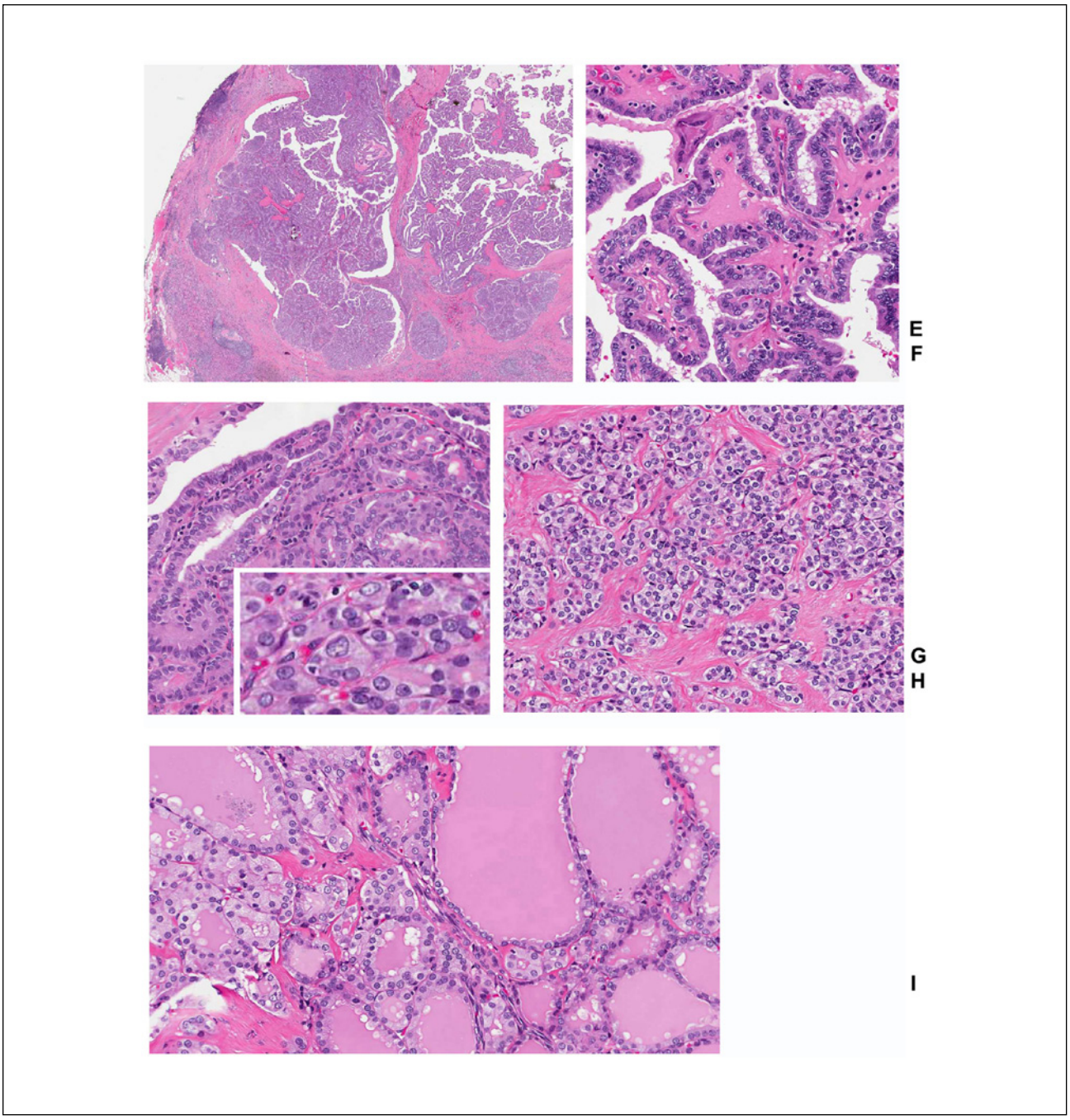

Figure 5. Total thyroidectomy for a multifocal and bilateral papillary thyroid carcinoma (PTC): (A, B, C, D, BB, and CC) Coronal sections of 4 giant sections and assembled hematoxylin and eosin–stained slides BB (section B) and CC (section C) revealed 2 large adjacent encapsulated tumor nodules in the right lobe (single and double arrows), 1 encapsulated nodule in the isthmus (single arrowhead), 1 encapsulated nodule of PTC in the left upper pole (double arrow), and 1 circumscribed but not encapsulated follicular variant of PTC in the middle of the left lobe (triple arrowhead). (E, F) Encapsulated PTC nodule with papillary architecture indicated by a single arrowhead in the isthmus. Note the multiple foci at the periphery, which may pose diagnostic problem in determining multifocality versus capsular invasion. (G) Encapsulated PTC nodule with papillary architecture indicated by a single arrowhead (in BB) in the isthmus. Inset: A high magnification showing focal oncocytic changes. (H) Encapsulated PTC in the left lobe indicted by double arrowhead in CC. Note the borderline nuclear changes for PTC. (I) Circumscribed but nonencapsulated nodule in the left lobe indicated by a triple arrowhead in CC showing a spectrum of nuclear changes ranging from normal to nuclear changes of PTC.

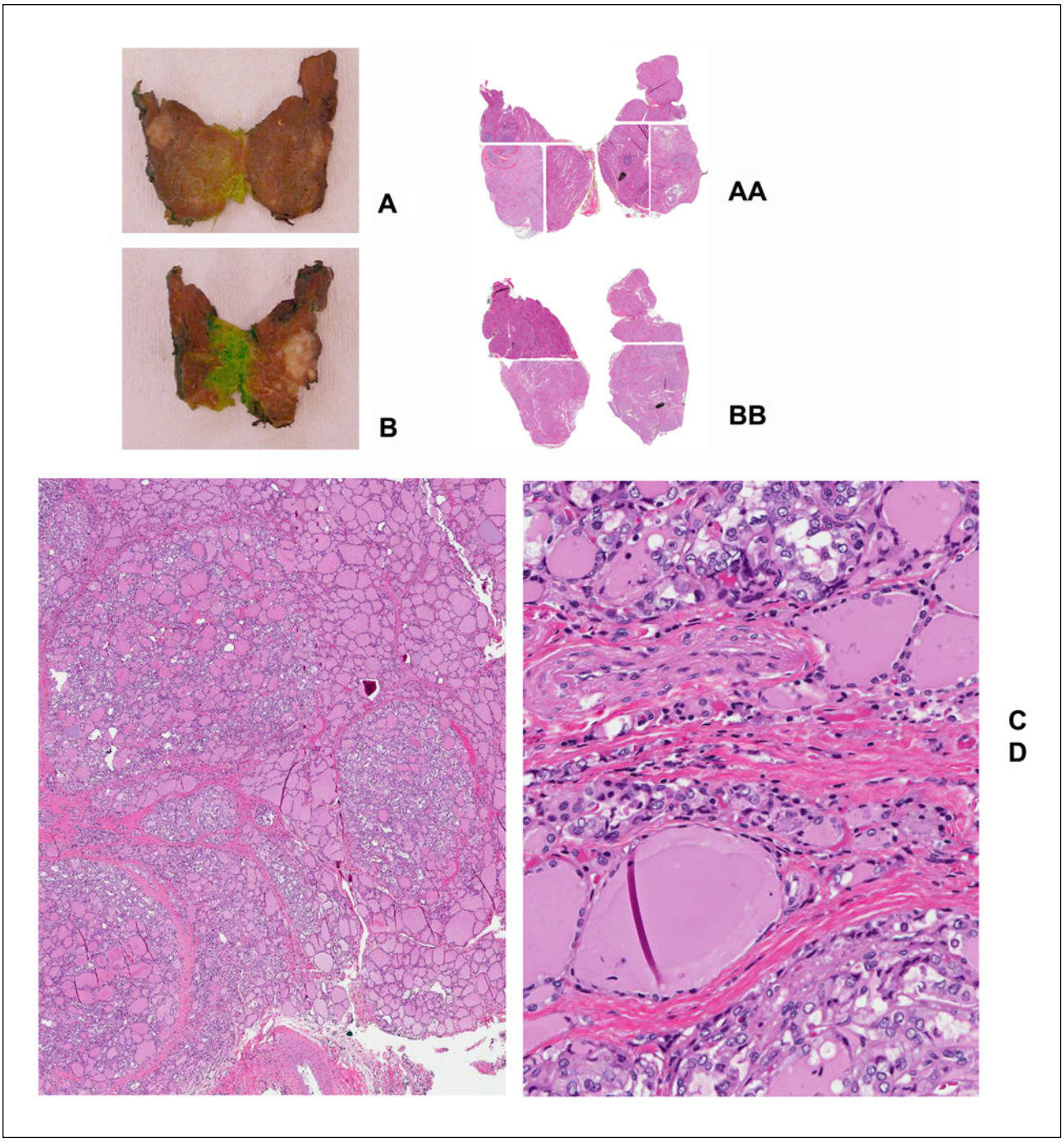

Figure 6. Total thyroidectomy for a multifocal and bilateral papillary thyroid carcinoma (PTC): (A, B, AA and BB) Coronal sections and assembled hematoxylin and eosin–stained slides showing the largest PTC nodule in the left lobe, second largest PTC nodule in the right lobe, and smaller nodules adjacent to and distant from the largest nodule. (C) The largest tumor in the left lobe surrounded by a cluster of smaller tumor nodules in the lower half of the left lobe. The largest tumor nodule appears to develop as a result of fusion of many small nodules surrounded by fibrous bands of tissue. (D) A high magnification of an area in C.

and a more aggressive behavior, including extrathyroidal extension, anaplastic transformation, and more advanced stage at presentation.[16,17,30] RET/PTC gene rearrangements are found in approximately 20% of sporadic PTC and are the most common alterations in radiation-induced PTC.[18,27] PTCs that harbor this genetic aberration typically have a classic papillary histology, a high rate of lymph nodal metastases but a low clinical stage at presentation, and

Table 2. Summary of the Distribution of Papillary Thyroid Carcinoma Foci According to Tumor Size.[a,b]

Diameter (mm)	Single Nodule	Single Nodule With Adjacent Cluster	Second Large Nodule or Random Foci	Total	Lymphatic Invasion	Isthmus Involved in Bilaterality
<10	11	5	3	19	0	1
10-20	14	13	25	52	4	4
>20	12	12	30	54	7	10
Total	37 (29.6%) [2] [1.6%]	30 (24.0%) [3] [2.4%]	58 (46.4%) [39] [31.2%]	125 (100%) [44] [35.2%]	11 (9.6%) [4] [9%]	15 (34.1%)[c]

[a]The difference in rates of bilaterality between tumors <10 mm and >10 mm was statistically significant ($P < .01$). The difference in rates of lymph nodal metastasis between tumors <10 mm and >10 mm was not statistically significant ($P = .1$).
[b]Figure in brackets indicates number of cases with bilateral involvement.
[c]Percentage calculated from cases with bilateral involvement of the thyroid.

appear to lack the predisposition for progression to poorly differentiated and anaplastic carcinomas.[16,19] Point mutations in the RAS gene, found in 10% to 15% of PTCs, are typically associated with follicular lesions of the thyroid including follicular carcinomas, and follicular adenomas. They are almost always found in the follicular variant of PTC. Other histopathologic features associated with RAS point mutations include tumor encapsulation and less prominent nuclear features of PTC.[5,16] In this study, molecular analyses were not performed to confirmed the above findings.

Examination of the coronally sectioned thyroid gland facilitated the panoramic and 3-dimensional visualization of different PTC foci. Of the 125 cases, multifocality/ multicentricity and bilaterality were observed in 70% and 35% cases, respectively. Encapsulated tumors had the largest mean tumor diameter and were associated with the lowest rate of multifocality/multicentricity as compared with the UV and TCV groups. For the EN group, a single nodule in one thyroid lobe, even when accompanied by satellite PTC foci adjacent to the main tumor mass, was associated with bilaterality in only 2 cases. In these 2 cases, the contralateral tumors were incidentally found microscopic PTC without aggressive histologic features, which are usually clinically insignificant.[20] This low rate of multifocality is also observed in follicular carcinomas, which are known to be associated with mutations in the RAS oncogene.

High rates of bilaterality were observed in UV and TCV groups associated with random PTC foci and >10 mm in maximum dimension as well as the EN group > 20 mm associated with random PTC foci. Moreover, lobectomy specimens in this study that had PTC with the above characteristics were frequently associated with PTC in the contralateral lobe of the completion thyroidectomy specimen.

The mechanism of multifocality/multicentricity of PTC has remained controversial despite clonality studies of different PTC foci. Some studies have demonstrated monoclonality of these foci, suggesting intraglandular spread as the mechanism of multifocality.[8,9] These studies were limited by technical specificity, and sensitivity, sampling problems, and interpretation of the results. Studies of X chromosome inactivation are limited by the natural monoclonal embryonal patch size in the normal thyroid.[11]

In other studies, in addition to PTC foci sharing clonality with the main tumor nodule, foci of different clonality have been demonstrated. Shattuck et al[14] found that up to 50% of multifocal PTC are of different clonal origin, thus representing independent primary tumors rather than intraglandular spread. In addition, different tumor nodules within one gland have been shown to have distinct genetic alterations, including diverse RET/PTC profiles and discordant patterns of BRAF mutations.[10,12] These findings suggest that these multifocal tumors arise independently in a background of genetic or environmental susceptibility.[10]

Therefore, multicentricity (different PTC foci of different clones) or multicentricity combined with multifocality (intraglandular lymphatic spread) play important roles in the formation of multiple PTC foci, particularly in that of the controlateral PTC. Although there is evidence lending strong support for mutmultifocality (multiple tumor within same lobe, satellite tumor in vicinity of the main tumor and associated metastatic tumor in lymph nodes and some identical molecular changes), our study of morphological and topographic mapping of PTC showed other evidences in favor of multicentricity[12-14,33-37]:

(a) Secondary PTC nodules located at the periphery or at a distance from the largest tumor mass may display histopathological features different from the main tumor nodule (ie, TCV, oncocytic features, papillary or follicular architecture, and foci of PTC with lower or borderline proportion of nuclear grooves and pseudo-inclusions).
(b) The absence of lymph nodal metastases and rare lymphatic invasion in the EN group despite the

presence of multifocality. The nodules of the EN group are often low in lymphatic vessel density.[36] Lymphatic invasion was rarely seen in multifical/bilateral PTC.

(c) The main PTC nodule and/or secondary (smaller) PTC foci were associated with nuclear changes that were borderline for the diagnosis of PTC, and therefore, it is doubtful that these tumors have the potential for lymphatic invasion.

(d) Isthmic involvement is not frequent in bilateral PTC. Intraglandular lymphatic spread to the contralateral lobe should be associated with tumor deposition in the isthmus.

(e) Thyroid tissue beyond the main tumor has the potential to develop de novo and independent PTC foci, particularly, incidental microscopic PTC.

Furthermore, in the EN group, satellite PTC foci adjacent to the main tumor nodule may mimic capsular invasion due to the attachment of the satellite tumor nodule to the capsule. Multifocality/multicentricity is favored over capsular invasion when (*a*) nodules are multiple, (*b*) nodules are of a large size, (*c*) capsular penetration is absent, and (*d*) nuclear changes are borderline for the diagnosis of PTC. As a result, the EN of PTC with a lobulated cross appearance likely develops from fusion of the main tumor with the adjacent satellite tumor nodule (Figures 3 and 4). Of interest, in this study, there was a large proportion of TCV of small size, a previously reported finding of PTC <10 mm accounting for 16% of TCV versus 9.5% for non-TCV.[38] Our technique of coronal sectioning with panaromic/3-dimensional view was likely useful to accurately identify and distinguish the main focus of PTC from satellite foci. This may result in smaller tumor size of the largest tumoral focus in multifocal TCV as compared to tumor sizes examined in non-coronal sections.

In conclusion, serial coronal sectioning of the thyroid gland in this study allowed for the panoramic and 3-dimensional visualization of individual nodules or distinct foci of multifocal PTC. Two topographic patterns were identified as follows: (*a*) multifocality with satellite PTC foci near the main tumor nodule prone to fuse with the main tumor and (*b*) multicentricity or random distribution of PTC foci in one or both thyroid lobes. Bilaterality was frequently observed in tumors associated with random PTC foci, whereas, the EN group tended to be unilateral and was not associated with random foci.

Declaration of Conflicting Interests

The author(s) declared no potential conflicts of interest with respect to the research, authorship, and/or publication of this article.

Funding

The author(s) received no financial support for the research, authorship, and/or publication of this article.

References

1. Haselkorn T, Bernstein L, Preston-Martin S, Cozen W, Mack WJ. Descriptive epidemiology of thyroid cancer in Los Angeles County, 1972-1995. *Cancer Causes Control*. 2000;11:163-170.
2. Hodgson NC, Button J, Solorzano CC. Thyroid cancer: is the incidence still increasing? *Ann Surg Oncol*. 2004;11:1093-1097.
3. Mulla ZD, Margo CE. Primary malignancies of the thyroid: epidemiologic analysis of the Florida Cancer Data System registry. *Ann Epidemiol*. 2000;10:24-30.
4. VanderLaan W. The occurrence of carcinoma of the thyroid gland in autopsy material. *N Engl J Med*. 1947;237:221.
5. Burgess JR. Temporal trends for thyroid carcinoma in Australia: an increasing incidence of papillary thyroid carcinoma (1982-1997). *Thyroid*. 2002;12:141-149.
6. Liu S, Semenciw R, Ugnat AM, Mao Y. Increasing thyroid cancer incidence in Canada, 1970-1996: time trends and age-period-cohort effects. *Br J Cancer*. 2001;85:1335-1339.
7. Kilfoy BA, Zheng T, Holford TR, et al. International patterns and trends in thyroid cancer incidence, 1973-2002. *Cancer Causes Control*. 2009;20:525-531.
8. McCarthy RP, Wang M, Jones TD, Strate RW, Cheng L. Molecular evidence for the same clonal origin of multifocal papillary thyroid carcinoma. *Clin Cancer Res*. 2006;12:2414-2418.
9. Sugg SL, Ezzat S, Rosen IB, Freeman JL, Asa SL. Distinct multiple RET/PTC gene rearrangements in multifocal papillary thyroid neoplasia. *J Clin Endocrinol Metab*. 1998;83:4116-4122.
10. Wang W, Wang H, Teng X, et al. Clonal analysis of bilateral, recurrent, and metastatic papillary thyroid carcinomas. *Hum Pathol*. 2010;41:1299-1309.
11. Jovanovic L, Delahunt B, McIver B, Eberhardt NL, Grebe SK. Thyroid gland clonality revisited: the embryonal patch size of the normal human thyroid gland is very large, suggesting X-chromosome inactivation tumor clonality studies of thyroid tumors have to be interpreted with caution. *J Clin Endocrinol Metab*. 2003;88:3284-3291.
12. Giannini R, Ugolini C, Lupi C, et al. The heterogeneous distribution of BRAF mutation supports the independent clonal origin of distinct tumor foci in multifocal papillary thyroid carcinoma. *J Clin Endocrinol Metab*. 2007;92:3511-3516.
13. Kuhn E, Teller L, Piana S, Rosai J, Merino MJ. Different clonal origin of bilateral papillary thyroid carcinoma, with a review of the literature. *Endocr Pathol*. 2012;23:101-107.
14. Shattuck TM, Westra WH, Ladenson PW, Arnold A. Independent clonal origins of distinct tumor foci in multifocal papillary thyroid carcinoma. *N Engl J Med*. 2005;352:2406-2412.
15. Nikiforova MN, Kimura ET, Gandhi M, et al. BRAF mutations in thyroid tumors are restricted to papillary carcinomas and anaplastic or poorly differentiated carcinomas

arising from papillary carcinomas. *J Clin Endocrinol Metab*. 2003;88:5399-5404.
16. Adeniran AJ, Zhu Z, Gandhi M, et al. Correlation between genetic alterations and microscopic features, clinical manifestations, and prognostic characteristics of thyroid papillary carcinomas. *Am J Surg Pathol*. 2006;30:216-222.
17. Xing M, Westra WH, Tufano RP, et al. BRAF mutation predicts a poorer clinical prognosis for papillary thyroid cancer. *J Clin Endocrinol Metab*. 2005;90:6373-6379.
18. Nikiforov YE. RET/PTC rearrangement in thyroid tumors. *Endocr Pathol*. 2002;13:3-16.
19. Tallini G, Santoro M, Helie M, et al. RET/PTC oncogene activation defines a subset of papillary thyroid carcinomas lacking evidence of progression to poorly differentiated or undifferentiated tumor phenotypes. *Clin Cancer Res*. 1998;4:287-294.
20. Niemeier LA, Kuffner Akatsu H, et al. A combined molecular-pathologic score improves risk stratification of thyroid papillary microcarcinoma. *Cancer*. 2012;118:2069-2077.
21. Nikiforova MN, Lynch RA, Biddinger PW, et al. RAS point mutations and PAX8-PPAR gamma rearrangement in thyroid tumors: evidence for distinct molecular pathways in thyroid follicular carcinoma. *J Clin Endocrinol Metab*. 2003;88:2318-2326.
22. Giordano TJ, Kuick R, Thomas DG, et al. Molecular classification of papillary thyroid carcinoma: distinct BRAF, RAS, and RET/PTC mutation-specific gene expression profiles discovered by DNA microarray analysis. *Oncogene*. 2005;24:6646-6656.
23. Santoro A, Pannone G, Carosi MA, et al. BRAF mutation and RASSF1A expression in thyroid carcinoma of southern Italy. *J Cell Biochem*. 2013;114:1174-1182.
24. Santarpia L, Sherman SI, Marabotti A, Clayman GL, El-Naggar AK. Detection and molecular characterization of a novel BRAF activated domain mutation in follicular variant of papillary thyroid carcinoma. *Hum Pathol*. 2009;40:827-833.
25. Myers MB, McKim KL, Parsons BL. A subset of papillary thyroid carcinomas contain KRAS mutant subpopulations at levels above normal thyroid [published online August 28, 2012]. *Mol Carcinog*. doi:10.1002/mc.21953.
26. Durand S, Ferraro-Peyret C, Joufre M, et al. Molecular characteristics of papillary thyroid carcinomas without BRAF mutation or RET/PTC rearrangement: relationship with clinico-pathological features. *Endocr Relat Cancer*. 2009;16:467-481.
27. Henderson YC, Shellenberger TD, Williams MD, et al. High rate of BRAF and RET/PTC dual mutations associated with recurrent papillary thyroid carcinoma. *Clin Cancer Res*. 2009;15:485-491.
28. Li X, Abdel-Mageed AB, Kandil E. BRAF mutation in papillary thyroid carcinoma. *Int J Clin Exp Med*. 2012;5:310-315.
29. Eberhardt NL, Grebe SK, McIver B, Reddi HV. The role of the PAX8/PPARγ fusion oncogene in the pathogenesis of follicular thyroid cancer. *Mol Cell Endocrinol*. 2010;321:50-56.
30. Elisei R, Ugolini C, Viola D, et al. BRAF(V600E) mutation and outcome of patients with papillary thyroid carcinoma: a 15-year median follow-up study. *J Clin Endocrinol Metab*. 2008;93:3943-3949.
31. Guerra A, Sapio MR, Marotta V, et al. The primary occurrence of BRAF(V600E) is a rare clonal event in papillary thyroid carcinoma. *J Clin Endocrinol Metab*. 2012;97:517-524.
32. Jovanovic L, Delahunt B, McIver B, Eberhardt NL, Grebe SK. Most multifocal papillary thyroid carcinomas acquire genetic and morphotype diversity through subclonal evolution following the intra-glandular spread of the initial neoplastic clone. *J Pathol*. 2008;215:145-154.
33. Park SY, Park YJ, Lee YJ, et al. Analysis of differential BRAF(V600E) mutational status in multifocal papillary thyroid carcinoma: evidence of independent clonal origin in distinct tumor foci. *Cancer*. 2006;107:1831-1838.
34. Eloy C, Santos J, Soares P, Sobrinho-Simões M. Intratumoural lymph vessel density is related to presence of lymph node metastases and separates encapsulated from infiltrative papillary thyroid carcinoma. *Virchows Arch*. 2011;459:595-605.
35. Hall FT, Freeman JL, Asa SL, Jackson DG, Beasley NJ. Intratumoral lymphatics and lymph node metastases in papillary thyroid carcinoma. *Arch Otolaryngol Head Neck Surg*. 2003;129:716-719.
36. Koo BS, Lim HS, Lim YC, et al. Occult contralateral carcinoma in patients with unilateral papillary thyroid microcarcinoma. *Ann Surg Oncol*. 2010;17:1101-1105.
37. Moreno Egea A, Rodriguez Gonzalez JM, Sola Perez J, Soria Cogollos T, Parrilla Paricio P. Prognostic value of the tall cell variety of papillary cancer of the thyroid. *Eur J Surg Oncol*. 1993;19:517-521.
38. Michels JJ, Jacques M, Henry-Amar M, Bardet S. Prevalence and prognostic significance of tall cell variant of papillary thyroid carcinoma. *Hum Pathol*. 2007;38:212-219.